Available online at www.sciencedirect.com
ScienceDirect
Biochimica et Biophysica Acta 1767 (2007) 520–527
Biochimica et Biophysica Acta
BBA
www.elsevier.com/locate/bbabio

Spare quinones in the Q_B cavity of crystallized photosystem II from *Thermosynechococcus elongatus*

Roland Krivanek [a], Jan Kern [b], Athina Zouni [b], Holger Dau [a,*,1], Michael Haumann [a,*]

[a] *Freie Universität Berlin, FB Physik, Arnimallee 14, D-14195 Berlin, Germany*
[b] *Technische Universität Berlin, Institut für Chemie, Sekr. PC14, Max-Volmer-Laboratorium für Biophysikalische Chemie, Straße des 17. Juni 135, D-10623 Berlin*

Received 15 November 2006; received in revised form 13 February 2007; accepted 19 February 2007
Available online 24 February 2007

Abstract

The recent crystallographic structure at 3.0 Å resolution of PSII from *Thermosynechococcus elongatus* has revealed a cavity in the protein which connects the membrane phase to the binding pocket of the secondary plastoquinone Q_B. The cavity may serve as a quinone diffusion pathway. By fluorescence methods, electron transfer at the donor and acceptor sides was investigated in the same membrane-free PSII core particle preparation from *T. elongatus* prior to and after crystallization; PSII membrane fragments from spinach were studied as a reference. The data suggest selective enrichment of those PSII centers in the crystal that are intact with respect to O_2 evolution at the manganese–calcium complex of water oxidation and with respect to the integrity of the quinone binding site. One and more functional quinone molecules (per PSII monomer) besides of Q_A and Q_B were found in the crystallized PSII. We propose that the extra quinones are located in the Q_B cavity and serve as a PSII intrinsic pool of electron acceptors.

Keywords: Chlorophyll fluorescence; Crystallization; Photosystem II; Quinone; Water oxidation

1. Introduction

Photosynthetic water oxidation is carried out by photosystem II (PSII), a multisubunit protein complex embedded in the thylakoid membranes of plants, algae, and cyanobacteria [1,2]. Two PSII form a homodimer as originally revealed by electron microscopy [3,4]. The absorption of sunlight by the chlorophylls of PSII powers the oxidation of water molecules at the manganese–calcium complex bound to the lumenal side of the D1-subunit of PSII, a unique reaction yielding the dioxygen of the atmosphere. The electrons derived from the Mn complex are transferred via a redox-active tyrosine (Y_Z) to two protein-bound plastoquinone (PQ) molecules at the reducing side of PSII. The eventually formed quinole feeds its electrons into the electron transfer (ET) chain of photosynthesis involving the cytochrome-b_6/f complex and PSI [2] and finally they are employed for carbon-dioxide fixation in the Calvin–Benson cycle generating carbohydrates.

After single-turnover excitation of PSII as provided, e.g., by a Laser flash, first the quinone denoted as Q_A which is tightly bound to the D2 subunit of PSII is reduced within <1 μs [5]. Thereafter, ET occurs from Q_A^- to Q_B which is bound to a site on the D1 subunit, on the hundreds of microseconds time scale [6]. After the second reduction of Q_A, somewhat slower ET to Q_B^- occurs, Q_B^{2-} is protonated, leaves its binding site in form of the quinole Q_BH_2, and an oxidized PQ molecule is bound [6]. The PQ exchange, at least in thylakoid membranes from plant material, clearly must be rapid because after only ~2 ms the electrons of Q_BH_2 serve to reduce the previously oxidized PSI [7,8].

The above sequence of events has been known for long. However, the problem has remained how the fast access of the

Abbreviations: β-DM, β-dodecylmaltoside; Chl, chlorophyll; DCBQ, 2,6-dichloro-p-benzoquinone; DF, delayed Chl fluorescence; ET, electron transfer; PF, prompt Chl fluorescence; PQ, plastoquinone; PSI/II, photosystem I/II; $Q_{A,B}$, plastoquinone molecules bound to the D2/D1 subunits of PSII; S_i, S-states of the Mn complex; Y_Z, the redox-active tyrosine-160/161 of the D1 subunit of PSII

* Corresponding authors. Tel.: +49 30 8385 6101; fax: +49 30 8385 6299.
E-mail addresses: holger.dau@physik.fu-berlin.de (H. Dau), haumann@physik.fu-berlin.de (M. Haumann).
[1] Tel.: +49 30 8385 3581.

0005-2728/$ - see front matter © 2007 Elsevier B.V. All rights reserved.
doi:10.1016/j.bbabio.2007.02.013

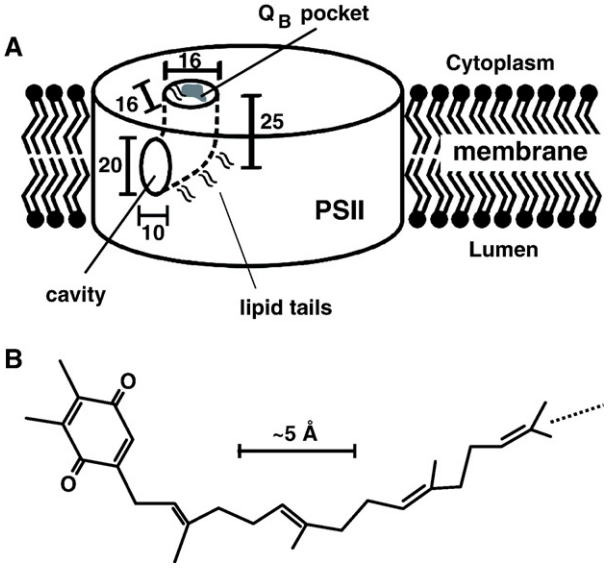

Fig. 1. (A) Schematic drawing of the cavity in the D1 subunit of PSII of *T. elongatus* that connects the membrane phase to the Q_B binding pocket as found in the crystal structure at 3 Å resolution (for details see [9]). Relative positions of the tails of lipids forming part of the wall of the cavity are indicated. Dimensions are approximate and given in Å (B) Structure of the plastoquinone molecule in the Q_B pocket as modeled on basis of the crystallographic data [9] (PDB entry 2AXT). Only the first four isoprenoid units of the PQ9 have been assigned.

bulky PQ molecules (amphiphilic 2,3-dimethyl-1,4-benzoquinone head, long hydrophobic tail of nine isoprenoid units (PQ9), Fig. 1B) to the Q_B binding pocket located in the interior of the PSII protein complex and the rapid release of Q_BH_2 to the membrane phase is realized.

The most recent crystallographic structure of PSII from *Thermosynechococcus elongatus* at 3 Å resolution [9] points to a solution of this problem. In this structure, at variance with a previous structure at lower resolution [10], most of the chlorophylls including their side chains as well as several carotenoid and lipid molecules have been assigned. Thus, it became feasible to assess more reliably the apparently unoccupied space in the protein. As a result, for the first time an apparent cavity starting at the protein boundary of the D1 protein facing the membrane and protruding up to the Q_B binding pocket has been uncovered [9].

In the crystallographic data [9], besides that of the Q_B molecule, there was no structured electron density in the cavity that could be attributed to quinone and/or lipid molecules. However, the size of the cavity seemingly was large enough to accommodate Q_B, one or more further quinones, and perhaps additional lipids (Fig. 1). Furthermore, lipid molecules were resolved in the structure which are attached to the D1 protein of PSII and some of them are placed in a way that their fatty acid chains coat parts of the wall of the cavity (Fig. 1). It is thus tempting to speculate that the cavity may provide a "lipid-lubricated" pathway for quinone diffusion from the membrane to the Q_B binding pocket and vice versa for quinole.

The question remains whether there are PQ molecules located in the cavity in the crystallized dimeric PSII which is devoid of the membrane due to detergent solubilization in the course of the purification. Even if present, such PQ may not be detectable in the crystallographic data due to disorder. Previous EPR experiments [11] and biochemical studies [12] indeed have provided evidence for the presence of more than one quinone in PSII core particles from *T. elongatus*. However, their functional relevance remained unclear.

In the present investigation we employed chlorophyll fluorescence as induced by light flashes to investigate electron transfer at both, the Mn complex of water oxidation and at the quinone-reducing side of PSII. The same oxygen-evolving PSII core particle preparation from *T. elongatus* as used previously for crystallographic data collection [9] was studied prior to and after crystallization and compared to PSII membrane fragments from spinach. Using delayed Chl fluorescence (DF) measurements [13], the ET at the Mn complex was characterized. Measurements of prompt Chl fluorescence (PF) [6,13] provided the number of electrons which were transferred at the reducing side of PSII and, thus, the number of PQ molecules that are functional and potentially located in the Q_B cavity.

2. Materials and methods

2.1. Sample preparation

PSII core particles from *T. elongatus* were purified as described in [12] and stored at −80 °C until use. This preparation preserves the native homodimeric structure of the PSII complex as visible in the crystallographic data [9]. One fraction of the crystallography-grade preparations was directly used for the measurements ($PSII_T^0$). From a second fraction of the preparations, crystals were grown as described in [12]. After careful redissolving of the crystals in a buffer (100 mM PIPES pH 7.0, 5 mM $CaCl_2$, 0.03% β-DM) [12], the resulting PSII samples were used for the measurements ($PSII_T^1$). The number of Chls per O_2 molecule was determined by single-flash oxygen evolution measurements [12,14]. Samples of PSII from *T. elongatus* containing ~1 mg/mL of Chl were diluted for the fluorescence measurements to 10 μg/mL of Chl in a buffer containing 1 M glycine betaine, 15 mM NaCl, 5 mM $MgCl_2$, 5 mM $CaCl_2$, 25 mM MES, pH=6.2 (buffer A) and in addition 0.03% β-DM. DCBQ (40 μM) was added as an artificial electron acceptor if applicable.

PSII membrane fragments from spinach ($PSII_S$) were prepared as outlined in [15] and stored at a Chl concentration of ~2 mg/mL at −80 °C until use. Their oxygen-evolution activity was ~1200 μmol O_2 (mg of Chl h)$^{-1}$ as determined on a Clark-type electrode at 28 °C. About 2 mL of the samples were thawed for ~1 h on ice, resuspended in ~200 mL of buffer A and collected by centrifugation (12 min, 4 °C, 20,000 rpm). The resulting pellet carefully was resuspended in buffer A at a Chl concentration of ~100 μg/mL and stored on ice until use. Samples for fluorescence measurements contained 10 μg/mL of Chl in buffer A and 20 μM DCBQ if not otherwise stated.

2.2. Prompt Chl fluorescence (PF) measurements

PF measurements were performed using a commercial double-modulation fluorometer (Photo Systems Instruments FL3000, Czech Republic) as previously [13]. The PF was excited by discrete weak light pulses from a diode array (λ ~ 620 nm, 8 μs duration) which were linearly spaced on a logarithmic time scale. Saturating excitation of samples was provided by a frequency-doubled Q-switched Nd:YAG Laser (Continuum Minilite II, λ=532 nm, FWHM=5 ns); the spacing between flashes was 0.7 s. Laser pulse intensities were adjusted to 2 mJ cm^{-2} (PSII membrane fragments) or 13 mJ cm^{-2} (PSII from *T. elongatus*) using the internal attenuator of the Laser and determined in parallel to the PF measurements by a meter (Ophir Optronics Nova, PE10 measuring head). The first data point was recorded at 76 μs after the excitation flash.

2.3. Delayed Chl fluorescence (DF) measurements

DF (recombination Chl fluorescence) was measured using a laboratory-built apparatus as outlined in [13,16,17]; the fluorescence was detected by a gated photomultiplier (Hamamatsu R2066, PMT Gated Socket Assembly C1392-55). Saturating flash excitation of samples was provided by the same Laser using the same pulse intensities and flash spacing interval as used for the PF measurements (see above). The DF was recorded in a time interval of 10 μs to 60 ms after each flash. DF signals were corrected for a small contribution of luminescence from the glass ware as described in [18].

2.4. Data evaluation

Fluorescence transients on each flash of a series of 32 flashes, after amplification (Tektronix AM502), were acquired on a PC equipped with a 12-bit 20 MHz A/D-card (ADLINK PCI9812) at a sampling frequency of 1 MHz using a home-made measuring program which employs an averaging procedure resulting in data points which are linearly spaced on a logarithmic time scale [18]. Data acquisition was started on each flash separately by a trigger pulse from a photodiode. In both PF and DF measurements, the excellent signal-to-noise ratio in principle allows for single-shot measurements. However, to improve the statistics, transients from three independent preparations of each type were averaged. The amplitudes and half-times of individual kinetic phases of the time-course of PF and DF transients were evaluated by simulations using a triple-exponential decay function plus an offset value. The magnitude of the millisecond component of DF transients was approximated by summation of data points in a time range of 1–4 ms after each flash [16].

3. Results and discussion

By delayed Chl fluorescence (DF) measurements [13], the rate and yield of the oxygen-evolving transition of the Mn complex [17–19] and the number of turnovers under flashing light were assessed. DF measurements were performed using three different PSII preparations. Membrane-free PSII core particles from the cyanobacterium *T. elongatus* prior to ($PSII_T^0$) and after crystallization ($PSII_T^1$) [12] were compared to PSII membrane fragments from spinach ($PSII_S$) [15].

DF transients on the first eight Laser flashes applied to dark-adapted samples in the presence and absence of the artificial electron acceptor DCBQ are shown in Fig. 2. The decay of the DF transients in the shown time range of 0.5–4 ms predominantly reflects electron transfer $Mn \rightarrow Y_Z^{\bullet +}$ on the O_2-evolving transition $S_3 \Rightarrow S_0$ [13,16,18]. Faster DF decay components (not shown) result from preceding relaxation processes likely involving proton movements [13,17,20]. In all three preparations, the O_2-evolving step occurred for the first time mainly on flash no. 3 as visible by the corresponding large DF amplitude, irrespective of the presence or absence of DCBQ, which indicates that the major fraction of PSII centers carried a Mn complex which was in its dark-stable S_1 state prior to the first flash.

The half-times ($t_{1/2}$) attributable to the O_2-evolving transition were derived from simulations of the DF transients on flash no. 3 (see Materials and methods and [13,16–20]). In the two PSII preparations from *T. elongatus*, $t_{1/2}$ was only slightly larger than that of 1.15 ms observed in $PSII_S$ (Table 1). The value of 1.15 ms is typical for the used highly active preparation [17,20–22]. The half-time of O_2 evolution is increased, e.g., when the extrinsic proteins [23] bound to the lumenal side of PSII are partially missing [24,39]. Accordingly, the main population of the PSII

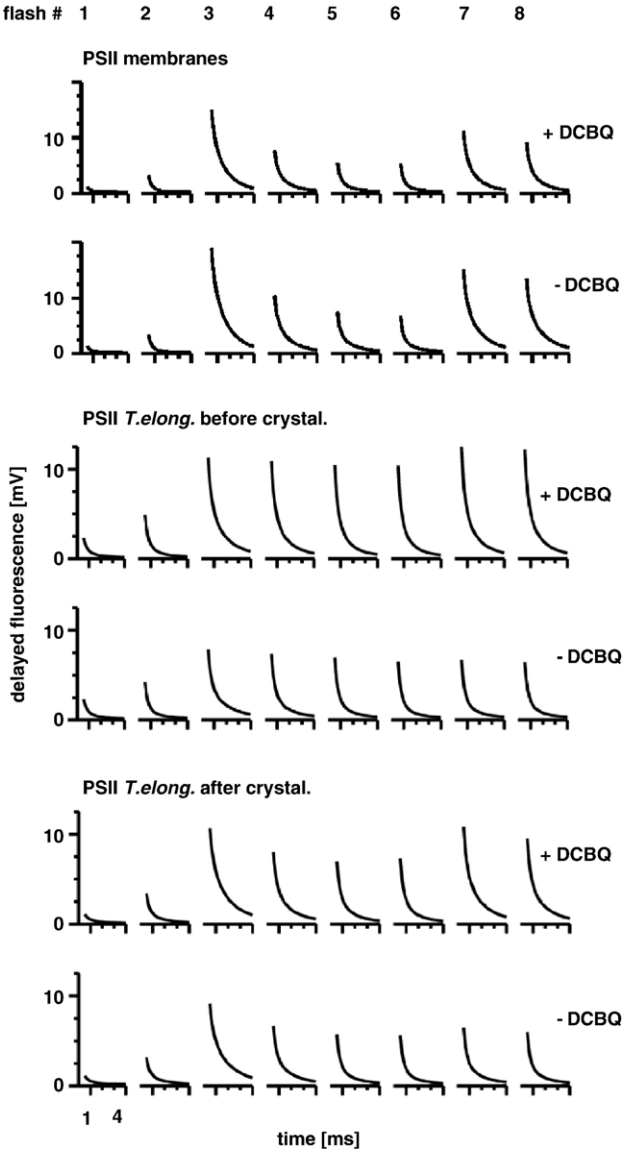

Fig. 2. Transients of delayed Chl fluorescence on flashes 1 to 8 given to dark-adapted PSII preparations in the presence (top) and absence (bottom) of DCBQ. The DF decay in the displayed time range of 0.5–4 ms after the flashes predominantly is attributable to electron transfer $Mn \rightarrow Y_Z^{\bullet +}$ on the oxygen-evolving transition. Data represent the average of three measurements on three independent preparations of each type.

preparations from *T. elongatus* was intact with respect to O_2 evolution and presumably also with respect to the content of the extrinsic proteins. A minor less intact population was clearly larger in $PSII_T^0$ than in $PSII_T^1$ as judged by the increased $t_{1/2}$ of O_2-formation of the former preparation. This result provides evidence that the intact PSII centers are accumulated in the crystals. In other words, the crystallization further purifies the PSII preparation by reducing the fraction of PSII which is less intact.

The magnitude of the millisecond DF component (Fig. 3, open squares) revealed an oscillation with a period of four in the presence of DCBQ. For these conditions, the unlimited electron acceptor capacity allowed for multiple turnovers of the four-stepped catalytic cycle of water oxidation. Superimposed to the

Table 1
Parameters which characterize the three PSII preparations

	PSII membrane fragments from spinach	PSII core particles from *T. elongatus*	
		Before crystal	After crystal
Chls per 1/4 O_2	~200[(a)]	60±7	55±7
$t_{1/2}$ of O_2-formation [ms]	1.15±0.1	1.45±0.1	1.25±0.1
Non-Q_B centers [%]	~20	~40	~30
Fraction of PSII centers with a single or more extra PQ	~100%	65–75%	70–80%

The number of Chls per released O_2 of PSII from *T. elongatus* was determined from single-flash oxygen evolution measurements; (a) the value for PSII membranes was adopted from [15]. The half-time of the O_2-evolving step was derived by simulation of the ms-phase of DF transients. The percentage of non-Q_B centers (upper limit) comes from the relative amplitude of the slowest PF phase on flash 1. The fraction of Q_B-containing PSII centers with one or more extra PQ was estimated from PF transients (see the text).

oscillating amplitude, a DF offset was present which rose to a maximum at higher flash numbers (Fig. 3, bars). The underlying slow DF decay possibly may be attributable (i) to a lack of the essential Ca ion, (ii) to a reduced content of one or several of the three extrinsic proteins, or (iii) to the absence of Mn. Any of these lesions may cause a slow DF phase on higher flash numbers [21,22] due to charge recombination between Q_A^- and Y_Z^+ or the Mn complex. In $PSII_S$ the respective portion of centers showing a slow DF decay phase was small (Fig. 3, bars), in line with the high O_2-activity. In $PSII_T^1$ this portion was much smaller than in $PSII_T^0$ again suggesting that those PSII centers which are intact with respect to donor side integrity are enriched in the crystals. Simulations (not shown) of the oscillations in the flash series of the millisecond DF amplitude (Fig. 3, open squares) [25] using the Kok-model of the S-state cycle [26], including the offset amplitude, and assuming an initial population of 100% S_1 yielded percentages of centers not hit by the flashes (misses, *M*) of 10% in $PSII_S$, 18% in $PSII_T^0$, and 15% in $PSII_T^1$, respectively. It is likely that the S_1-population had been close to 100% because of the extended dark-adaptation period prior to the measurements (preparation, storage, and thawing of samples in near darkness). Allowing for a maximal S_0 population of 25% in the simulations caused the miss factors to decrease, the above ordering with respect to the three PSII preparations was preserved. (We note that the amplitude of the millisecond DF component on flash 2 in the *T. elongatus* data (Fig. 3) likely is not attributable to the O_2-evolving transition, but rather to slower processes in PSII centers with a lesion at the donor side as discussed above.) The higher miss factor in $PSII_T$ (in comparison to $PSII_S$) presumably was attributable to the flash illumination which was not 100% saturating due to the smaller antenna size in the case of PSII from *T. elongatus*.

In the absence of DCBQ, the electron acceptor capacity of the reducing side of PSII is limited by the amount of quinone molecules which originally are present in the preparations. In $PSII_S$, because even the second maximum of the millisecond DF phase on flash no. 7 was visible (Figs. 2 and 3), at least seven single-electron turnovers were feasible. This number, taken at face value, corresponds to the full reduction of the initially bound Q_B, of two additional PQ molecules, and to the formation of Q_A^-. In $PSII_T^0$ the electron acceptor capacity was somewhat smaller than in $PSII_S$ as the second maximum on flash 7 of the millisecond DF phase was barely visible (Fig. 3, solid squares). In $PSII_T^1$, the second maximum of the millisecond DF was clearly visible although smaller than in $PSII_S$. These results suggest the presence of at least one additional PQ besides of Q_A and Q_B in the major fraction, but not in all centers, of the PSII preparation of *T. elongatus*. From the DF amplitudes, an estimate of the minimal number of PQ molecules per PSII was obtained because only completion of a full O_2-evolution cycle can be detected. Further characterization of the PQ content was derived from the monitoring of the ET at the reducing side of PSII employing measurements of the prompt Chl fluorescence (PF).

By PF measurements (Fig. 4), the oxidation of Q_A^- after Laser-flash excitation is monitored by the decay of the level of Chl fluorescence as excited by weak probe flashes [18,27]. Upon Q_A^- formation, the initial fluorescence (F_0^{ox}) rises to F_{max}^{ox}. If the PQ pool becomes reduced, both F_0^{ox} and F_{max}^{ox} are increased (to F_0^{red} and F_{max}^{red}) (Fig. 4B). This effect has been attributed to the partial quenching of the PF by oxidized quinones, contributing to the fluorescence induction curves ([28–30] and references therein). (In addition, the formation of the higher S-states slightly decreases the PF yield; see below.) The increase from F_{max}^{ox} to F_{max}^{red} was of similar magnitude

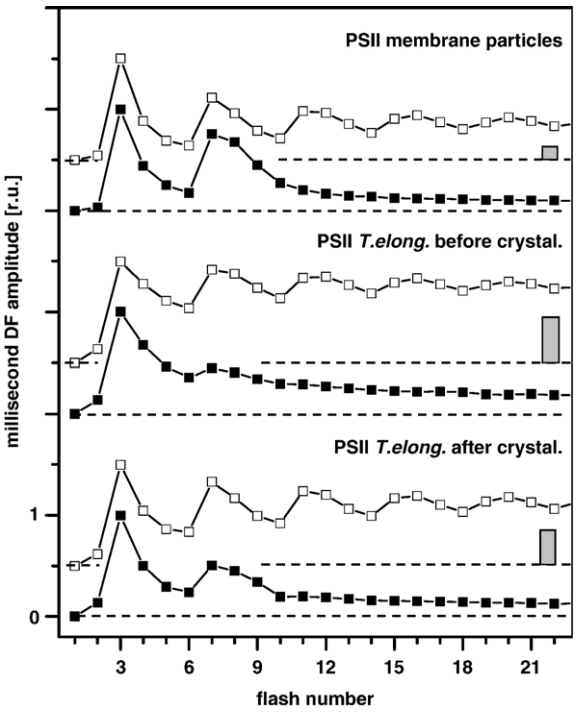

Fig. 3. The amplitudes of the millisecond component from DF data DF as function of the flash number. Open squares, +DCBQ; solid squares, −DCBQ. Amplitudes were determined by summation of the DF in the range of 0.5–4 ms after each flash and normalized to unity on the 3rd flash; the first flash amplitude was set to zero. Data sets are vertically displaced for comparison. Grey bars show the DF offset presumably attributable to impaired centers (see the text for details).

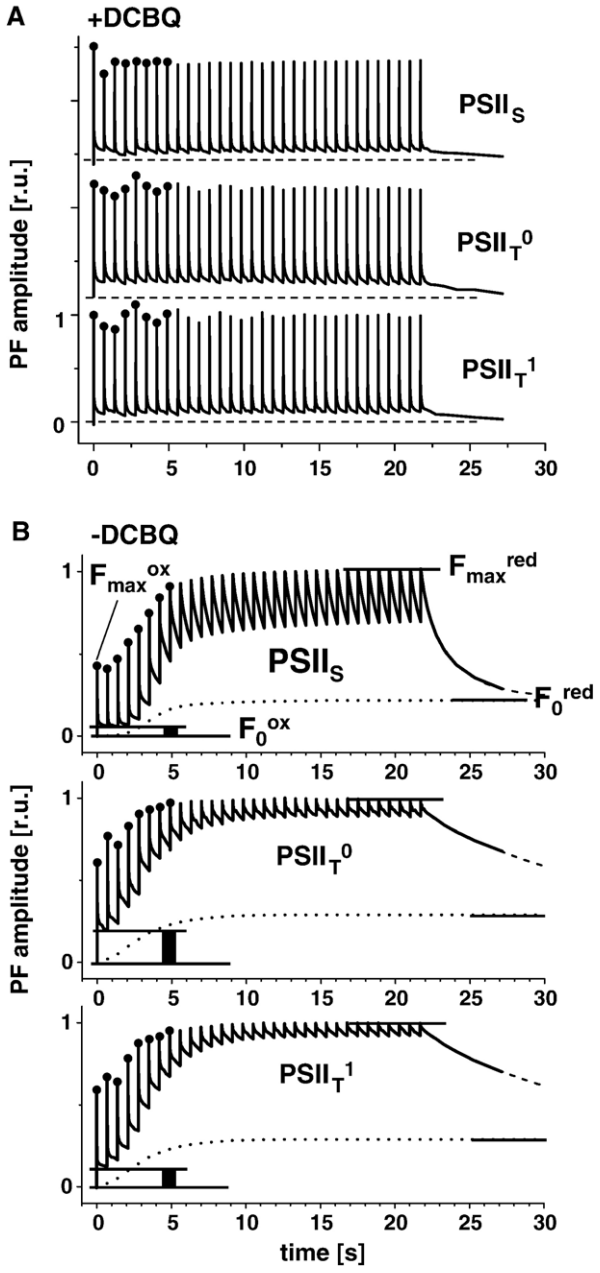

Fig. 4. Transients of prompt Chl fluorescence in a series of flashes given to the three PSII preparations in the presence (A) and absence (B) of DCBQ. The respective fluorescence levels discussed in the text are indicated. Black bars in (B) shows approximate proportions of non-Q_B centers. Dots highlight the oscillatory behavior of the initial PF amplitudes. Data represent the average of measurements on three independent preparations of each type.

in $PSII_S$ and $PSII_T$ (Fig. 4B), suggesting similar PQ-quenching of the PF perhaps due to a comparable PQ content in both preparations. We note that the observation of PQ-quenching in the membrane-free PSII-core particles suggests that the PQ-molecules associated with an individual PSII rather than the PQ-molecules in the membrane phase are responsible for the quenching effect.

The decay of the PF comprises at least three kinetic components [6,31]. (1) The most rapid decay phase is due to Q_A^- oxidation by electron transfer to Q_B, Q_B^-, or DCBQ on the hundreds of microseconds time scale. (2) An intermediate PF phase is due to centers where Q_B is not initially available, but becomes bound to its site within milliseconds. (3) Charge recombination between Q_A^- and the PSII donor side within hundreds of milliseconds to seconds contributes to the slowest PF decay. Accordingly, for a series of flash excitations of PSII, the number of PQ molecules per PSII can be estimated from the PF amplitudes of processes (1) and (2) which are associated with ET between the quinones.

Fig. 4A shows PF transients induced by 32 Laser flashes given to the three dark-adapted PSII preparations in the presence of DCBQ. Apparently, the decay from its initial maximum due to Q_A^- formation of the PF was rapid and almost quantitative on all flashes and in the three PSII samples. The small amplitude of the PF decay due to charge recombination which was visible after the last flash of the series indicates that the portion of centers in which Q_A^- was not accessible for rapid oxidation was ~10%. These results imply that, even when the Q_B binding site initially was unoccupied, the addition of DCBQ was sufficient to activate most centers. (It has been reported [45] that DCBQ may become reduced in the dark in a similar buffer as used here. Because the data in Fig. 4 clearly show that DCBQ was able to efficiently accept electrons, there is no evidence for significant dark-reduction of DCBQ in the present study).

Interestingly, a pronounced oscillation of the initial PF amplitude with period of four and a maximum on flash 1 and minimum on flash 3 was visible (Fig. 4A, dots) in the two preparations from *T. elongatus*. Presumably it is attributable to an S-state dependent PF yield (close to the F_0-level) or quenching by oxidized P_{680} (close to the F_{max}-level) as previously proposed ([28,32,47,48] and references therein). In the PSII membranes the PF was larger on flash 1 and minimal on flash 2, but oscillations were almost absent on higher flash numbers. A possible explanation for the different oscillatory behavior is that a period-of-two oscillation in the PF magnitude due to alternating electron transfer events $Q_A^- \rightarrow Q_B$ and $Q_A^- \rightarrow Q_B^-$ (see below) was superimposed to the quaternary oscillation due to the S-state cycling in the PSII membranes, but not in PSII from *T. elongatus*, because only in the core preparation Q_B was replaced by DCBQ. The pronounced S-state dependence of the PF in PSII of *T. elongatus* deserves in-depth analysis, but is not further assessed in the present study.

In the case of PSII from *T. elongatus*, the initial PF amplitudes in the absence of DCBQ revealed a binary oscillation with minimum on flash 1 and maximum on flash 2 (Fig. 4B, dots). The quaternary oscillation observed in the presence of DCBQ (Fig. 4A) was no longer detectable. In $PSII_S$ the flash-number dependent variations of the PF amplitudes were different. The PF amplitudes may reflect variations of the PF yield due to reactions at the quinone-reducing side or at the Mn complex. If the initial PF-yield was smaller upon formation of Q_A^- in the presence of Q_B than in the presence of Q_B^-, the oscillation of the initial PF amplitudes (Fig. 4B, dots) suggests that Q_B was largely oxidized prior to flash 1 in the PSII from *T. elongatus*.

An estimate of the numbers of electrons that were transferred at the reducing side of PSII was obtained from triple-exponential

simulations (not shown) of the data in Fig. 4B (see Materials and methods). (The respective apparent halftimes (see below) were considerably longer than those in thylakoids from plant material [6,8,31] and in the non-oxygenic, but structurally related reaction center of purple bacteria [33,34]; an effect of the detergent on the quinone-reducing side of PSII cannot be excluded.) The total PF decay due to ET between the quinones was derived by summation of the amplitudes of the two most rapid PF phases with halftimes in the range of 0.5–2 ms and 5–20 ms, respectively. The mean half-time of charge recombination resulted from a biexponential fit plus offset of the PF decay after the last flash of the series. It was ~0.8 s in $PSII_s$ and larger (~2.8 s) in $PSII_T$. The offset magnitude was assumed to represent the F_0^{red} level (Fig. 4B, dotted lines). The sum of the amplitudes of the first two PF decay phases was normalized on the respective difference ($F_{max} - F_0$) on each flash. The resulting relative amplitudes as function of the flash number are shown in Fig. 5.

In $PSII_S$, the PF decay due to ET between the quinones amounted to ~80% of the total amplitude on the first two flashes, the respective values were ~60% in $PSII_T^0$ and ~75% in $PSII_T^1$. The remaining PF mainly decayed by charge recombination in non-Q_B centers. Accordingly, the population of such centers was diminished in the crystallized PSII from *T. elongatus* and amounted to less than 30%. On higher flash numbers, the relative amplitude of the rapid PF decay decreased (Fig. 5) due to exhaustion of oxidizable PQ molecules. That this decrease was steeper in $PSII_S$ than in $PSII_T^1$ may reflect the increased miss factor in the latter preparation or movement of quinones between PSII centers in the membrane of the $PSII_S$ preparation.

In the following the data of Fig. 5 are discussed in more detail for the $PSII_T^1$, i. e. the PSII core complexes after crystallization. As outlined above, 70–75% of these contain at least one functional Q_B-type quinone besides Q_A, as indicated by the value of PF_{rapid} for the first two flashes. We estimate that of these close to 80% contain two quinones besides Q_A, because the PF_{rapid}-value for the third and fourth flash is by ~20% lower than for the first and second flash. The values for the fifth and sixth flash indicate that most likely a fraction of PSII contains even three functional PQ in addition to Q_A. Quantification of this fraction is hampered by the influence of miss events and slow charge recombination in the PSII with exhausted PQ pool. We roughly estimate that 20–35% of the $PSII_T^1$ contain a pool of three PQ molecules. The above numbers suggest that each PSII on the average contains close to three quinones (Q_A and Q_B-pool) which agrees with the 2.9±0.8 quinones per PSII previously found by liquid chromatography [12]. In the $PSII_T^0$ the number of functional quinones per PSII may be slightly smaller, in $PSII_S$ slightly greater than in $PSII_T^1$ (Table 1).

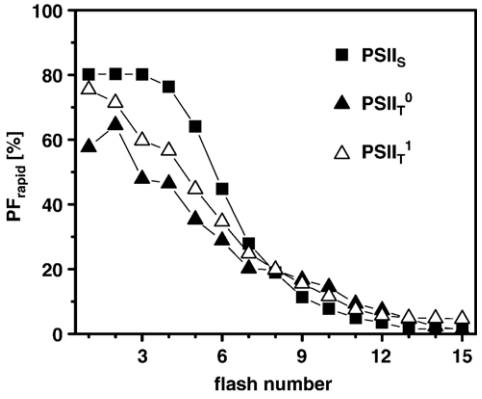

Fig. 5. The sum of the relative amplitudes of the two rapid PF decay phases of the three PSII preparations for the first 15 flashes. From these data, the fraction of PSII which transfers an electron from Q_A to Q_B can be estimated (for each flash).

In the above analysis of the PF data (Figs. 4 and 5) we implicitly assumed that the PF magnitude is linearly related to the amount of PSII centers with reduced Q_A (closed centers). This assumption is only approximately valid due to excitation energy transfer from PSII with reduced Q_A to PSII with oxidized Q_A, a phenomenon denoted as PSII connectivity (see [28,43]). The effect is that the fluorescence level for a given fraction of closed centers is smaller than expected for a linear relation. Thus, in the above considerations, the extent of the kinetic components reflecting electron transfer between the quinones may be slightly overestimated. In the case of the dissolved PSII core particles from *T. elongatus* excitation energy transfer between PSII dimers is almost negligible [46] and thus the influence of connectivity likely is small. In line with this notion, the estimated PQ content is similar to previous estimates [12]. In the used PSII membranes connectivity has been quantified previously and also is relatively small ($p=0.319$) [13]. Accordingly, the average PQ pool size found here for PSII membranes of 2–3 PQ per PSII (besides of Q_A) will be close to the real value. This PQ pool is considerably smaller than that (~6 PQ per PSII) determined for PSII in thylakoids [38,44]. Seemingly, some quinones were extracted during the detergent treatment in the preparation of the PSII membranes.

A fully quantitative determination of the PQ distribution among PSII centers from the fluorescence data may be experimentally feasible (see, e.g., [43]), but is not straightforward and beyond the scope of the present work. Future studies along this line may result in further insights into the mechanism underlying the retention of quinone [41].

4. Conclusions

Investigation of the ET reactions at the donor and acceptor sides of PSII core particles from *T. elongatus* [9,12] in comparison to PSII membrane fragments from spinach using Chl fluorescence techniques provides insights into the integrity, functional competence, and PQ content of the reaction centers. The obtained results are summarized as follows.

(1) PSII core particles from *T. elongatus* which previously have been crystallized were compared to the same preparation before crystallization. The crystallized PSII contains less non-Q_B centers and shows a smaller half-time of oxygen-evolution which is more similar to that of the highly intact PSII membranes than the non-crystallized PSII. A slightly lower Chl content, but higher PQ content was determined in the former samples. Accordingly, the PSII in the crystals seems to

be more intact with respect to the Mn complex of water oxidation (e.g. presence of the three extrinsic proteins, Mn, and Ca) and to the quinone binding site. These results suggest that the intact PSII is selectively enriched in the crystals.

(2) Approximately two PQ molecules besides of Q_A are, on the average, reducible in the crystallized core particles from *T. elongatus*. The majority fraction of PSII seems to contain two Q_B, whereas sizable minority fractions contain either none or three functional quinones besides Q_A. That more than one Q_B is present, is in line with previous studies [11,12,35]. The total value of about three PQ molecules per PSII center is in agreement with the 2.9±0.8 PQ per PSII found earlier in the same preparation [12]. We show here that this PQ is functional. As the membrane is absent in the core particles, we hypothesize that the spare PQ is located in the cavity pointing to the Q_B-site [9]. It is worth to note that several PQ molecules also have been found in PSII core preparations from other cyanobacteria [36,37]. If there is a similar cavity as in the cyanobacterial PSII in the plant material, it may also contain minimally two PQ molecules. However, the PQ content of PSII membranes seems to depend on the particular type of preparation [38]. We note that induction of the four steps of the catalytic cycle of water oxidation by four flashes, may not require the addition of artificial electron acceptors even in non-membraneous PSII preparations. Thus, in principle, by flash-illumination higher S-states can be reached in PSII crystals and studied crystallographically.

(3) The association of superstoichiometric numbers of quinone molecules with membrane protein complexes previously has been described, e.g., in the case of the bacterial RC–LH1 complex of *Rhodobacter sphaeroides* [40,41] and in proteins of the mitochondrial respiratory chain [42] and the formation of a quinone-rich phase at the membrane–protein interface involving both quinone–protein and quinone–quinone interactions has been discussed [41]. In the light of the crystallographic findings [9], one interpretation of the results in the present work is that at least in photosystem II, the efficient replacement of quinones for electron transfer further may require more specific structural determinants, namely the Q_B cavity connecting the membrane phase to the Q_B site.

In conclusion, we have observed extra PQ molecules in the three PSII preparations. Specifically in the previously crystallized PSII core particles it is unlikely that the quinones are attached to the periphery of PSII. Thus, we propose that these quinones are located in the Q_B cavity, supporting the previous suggestion [9] that there is a specific diffusion path for PQ between the membrane phase and the Q_B binding pocket. The extra PQ may function as a buffer. By the rapid exchange of Q_BH_2 against one of the PQ molecules in the cavity, the capability of PSII to transfer electrons at the acceptor side quickly would be restored.

Acknowledgements

Financial support by the Volkswagen-Foundation (grant I/77–575), the Deutsche Forschungsgemeinschaft within SFB 498 (projects C6, C8, C7), and the Bundesministerium für Bildung und Forschung (Consortium “Grundlagen für einen biomimetischen und biotechnologischen Ansatz der Wasserstoffproduktion”, grant 035F0318C) is gratefully acknowledged.

References

[1] J.H.A. Nugent (Ed.), Photosynthetic Water oxidation (special issue), Biochim. Biophys. Acta, 1503, 2001, pp. 1–259.
[2] N. Nelson, C.F. Yocum, Structure and function of photosystems I and II, Annu. Rev. Plant Biol. 57 (2006) 521–567.
[3] S. Iwata, J. Barber, Structure of photosystem II and molecular architecture of the oxygen-evolving centre, Curr. Opin. Struct. Biol. 14 (2004) 447–453.
[4] J. Barber, Photosystem II: the engine of life, Q. Rev. Biophys. 36 (2003) 71–89.
[5] A.R. Holzwarth, M.G. Muller, M. Reus, M. Nowaczyk, J. Sander, M. Rögner, Kinetics and mechanism of electron transfer in intact photosystem II and in the isolated reaction center: pheophytin is the primary electron acceptor, Proc. Natl. Acad. Sci. U. S. A. 103 (2006) 6895–6900.
[6] R. de Wijn, H.J. van Gorkom, Kinetics of electron transfer from QA to QB in photosystem II, Biochemistry 40 (2001) 11912–11922.
[7] W. Haehnel, The reduction kinetics of chlorophyll aI as an indicator for proton uptake between the light reactions in chloroplasts, Biochim. Biophys. Acta 440 (1976) 506–521.
[8] M. Haumann, W. Junge, The rates of proton uptake and electron transfer at the reducing side of photosystem II in thylakoids, FEBS Lett. 347 (1994) 45–50.
[9] B. Loll, J. Kern, W. Saenger, A. Zouni, J. Biesiadka, Towards complete cofactor arrangement in the 3.0 A resolution structure of photosystem II, Nature 438 (2005) 1040–1044.
[10] K.N. Ferreira, T.M. Iverson, K. Maghlaoui, J. Barber, S. Iwata, Architecture of the photosynthetic oxygen-evolving center, Science 303 (2004) 1831–1838.
[11] C. Fufezan, C. Zhang, A. Krieger-Liszkay, A.W. Rutherford, Secondary quinone in photosystem II of *Thermosynechococcus elongatus*: semiquinone-iron EPR signals and temperature dependence of electron transfer, Biochemistry 44 (2005) 12780–12789.
[12] J. Kern, B. Loll, C. Lüneberg, D. DiFiore, J. Biesiadka, K.-D. Irrgang, A. Zouni, Purification, characterization, and crystallization of photosystem II from *Thermosynechococcus elongatus* cultivated in a new type of photobioreactor, Biochim. Biophys. Acta 1706 (2005) 147–157.
[13] M. Grabolle, H. Dau, Energetics of primary and secondary electron transfer in photosystem II membrane particles of spinach revisited on basis of recombination-fluorescence measurements, Biochim. Biophys. Acta 1708 (2005) 209–218.
[14] S. Isgandarova, G. Renger, J. Messinger, Functional differences of photosystem II from *Synechococcus elongatus* and spinach characterized by flash induced oxygen evolution patterns, Biochemistry 42 (2003) 8929–8938.
[15] H. Schiller, H. Dau, Preparation protocols for high-activity Photosystem II membrane particles of green algae and higher plants, pH dependence of oxygen evolution and comparison of the S2-state multiline signal by X-band EPR spectroscopy, J. Photochem. Photobiol., B 55 (2000) 138–144.
[16] J. Clausen, W. Junge, H. Dau, M. Haumann, Photosynthetic water oxidation at high O_2 backpressure monitored by delayed chlorophyll fluorescence, Biochemistry 44 (2005) 12775–12779.
[17] J. Buchta, M. Grabolle, H. Dau, Photosynthetic dioxygen formation studied by time-resolved delayed fluorescence measurements -method, rationale, and results on the activation energy of dioxygen formation, Biochim. Biophys. Acta 1767 (2007) 565–574 (this issue).
[18] M. Grabolle, Die Donorseite des Photosystems II: Rekombinationsfluoreszenz- und Röntgenabsorptionsstudien. PhD thesis (2005) FU Berlin.
[19] M. Haumann, M. Barra, P. Loja, S. Löscher, R. Krivanek, A. Grundmeier, L.E. Andreasson, H. Dau, Bromide does not bind to the Mn(4)Ca complex in its S(1) state in Cl(−)-depleted and Br(−)-reconstituted oxygen-evolving photosystem II: evidence from X-ray absorption spectroscopy at the Br K-edge, Biochemistry 45 (2006) 13101–13107.
[20] M. Haumann, P. Liebisch, C. Müller, M. Barra, M. Grabolle, H. Dau,

Photosynthetic O_2 formation tracked by time-resolved X-ray experiments, Science 310 (2005) 1019–1021.
[21] M. Barra, M. Haumann, P. Loja, R. Krivanek, A. Grundmeier, H. Dau, Intermediates in assembly by photoactivation after thermally accelerated disassembly of the manganese complex of photosynthetic water oxidation, Biochemistry 45 (2006) 14523–14532.
[22] M. Barra, M. Haumann, H. Dau, Specific loss of the extrinsic 18 KDa protein from photosystem II upon heating to 47 °C causes inactivation of oxygen evolution likely due to Ca release from the Mn-complex, Photosynth. Res. 84 (2005) 231–237.
[23] A. Seidler, The extrinsic polypeptides of photosystem II, Biochim. Biophys. Acta 1277 (1996) 35–60.
[24] M. Haumann, M. Hundelt, P. Jahns, S. Chroni, O. Bögershausen, D. Ghanotakis, W. Junge, Proton release from water oxidation by photosystem II: similar stoichiometries are stabilized in thylakoids and PSII core particles by glycerol, FEBS Lett. 410 (1997) 243–248.
[25] R. de Wijn, H.J. van Gorkom, S-state dependence of the miss probability in photosystem II, Photosynth. Res. 72 (2002) 217–222.
[26] B. Kok, B. Forbush, M. McGloin, Cooperation of charges in photosynthetic O2 evolution—I. A linear four-step mechanism, Photochem. Photobiol. 11 (1970) 457–475.
[27] P. Pospisil, H. Dau, Chlorophyll fluorescence transients of Photosystem II membrane particles as a tool for studying photosynthetic oxygen evolution, Photosynth. Res. 65 (2000) 41–52.
[28] H. Dau, Molecular mechanisms and quantitative models of variable photosystem II fluorescence, Photochem. Photobiol. 60 (1994) 1–23.
[29] D. Lazar, Chlorophyll a fluorescence induction, Biochim. Biophys. Acta 1412 (1999) 1–28.
[30] H. Dau, Short-term adaptation of plants to changing light intensities and its relation to photosystem II photochemistry and fluorescence emission, J. Photochem. Photobiol. B 26 (1994) 3–27.
[31] A.R. Crofts, C.A. Wraight, The electrochemical domain of photosynthesis, Biochim. Biophys. Acta 726 (1983) 149–185.
[32] N. Steffen, G. Christen, G. Renger, Time-resolved monitoring of flash-induced changes of fluorescence quantum yield and decay of delayed light emission in oxygen-evolving photosynthetic organisms, Biochemistry 40 (2001) 173–180.
[33] A. Remy, K. Gerwert, Coupling of light-induced electron transfer to proton uptake in photosynthesis, Nat. Struct. Biol. 10 (2003) 637–644.
[34] S. Hermes, O. Bremm, F. Garczarek, V. Derrien, P. Liebisch, P. Loja, P. Sebban, K. Gerwert, M. Haumann, A time-resolved iron-specific X-ray absorption experiment yields no evidence for an Fe2+–Fe3+ transition during QA–QB electron transfer in the photosynthetic reaction center, Biochemistry 45 (2006) 353–359.
[35] K. Zimmermann, M. Heck, J. Frank, J. Kern, I. Vass, A. Zouni, Herbicide binding and thermal stability of photosystem II isolated from *Thermosynechococcus elongatus*, Biochim. Biophys. Acta 57 (2006) 106–114.
[36] X.-S. Tang, B.A. Diner, Biochemical and spectroscopic characterization of a new oxygen-evolving photosystem II core complex from the cyanobacterium *Synechocystis PCC 6803*, Biochemistry 33 (1994) 4594–4603.
[37] T. Ono, K. Satoh, S. Katoh, Chemical composition of purified oxygen-evolving complexes from the thermophilic cyanobacterium *Synechococcus spec*, Biochim. Biophys. Acta 852 (1986) 1–8.
[38] J. Kurreck, R. Schodel, G. Renger, Investigation of the plastoquinone pool size and fluorescence quenching in thylakoid membranes and Photosystem II membrane fragments, Photosynth. Res. 63 (2000) 171–182.
[39] M. Miyao, N. Murata, J. Lavorel, B. Maison-Peteri, A. Boussac, A.-L. Etienne, Effect of the 33-kDa protein on the S-state transitions in photosynthetic oxygen evolution, Biochim. Biophys. Acta 890 (1987) 151–159.
[40] F. Francia, M. Dezi, R. Rebecchi, A. Mallardi, G. Palazzo, B.A. Melandir, G. Venturoli, Light-harvesting complex I stabilizes $P^+Q_B^-$ charge separation in reaction centers of *Rhodobacter sphaeroides*, Biochemistry 43 (2004) 14199–14210.
[41] F. Comayras, C. Jungas, J. Lavergne, Functional consequences of the organization of the photosynthetic apparatus in *Rhodobacter sphaeroides*, J. Biol. Chem. 280 (2005) 11203–11213.
[42] A. Lass, R.S. Sohal, Comparisons of coenzyme Q bound to mitochondrial membrane proteins among different mammalian species, Free Radic. Biol. Med. 27 (1999) 220–226.
[43] J. Lavergne, J.-P. Bouchaud, P. Joliot, Plastoquinone compartmentation in chloroplasts. II. Theoretical aspects, Biochim. Biophys. Acta 1101 (1992) 13–22.
[44] P. Joliot, J. Lavergne, D. Beal, Plastoquinone compartmentation in chloroplasts. I: evidence for domains with different rates of photoreduction, Biochim. Biophys. Acta 1101 (1992) 1–12.
[45] A. Boussac, F. Rappaport, P. Carrier, J.M. Verbavatz, R. Gobin, D. Kiriliovsky, A.W. Rutherford, M. Sugiura, Biosynthetic Ca2+/Sr2+ exchange in the photosystem II oxygen-evolving enzyme of *Thermosynechococcus elongatus*, J. Biol. Chem. 279 (2004) 22809–22819.
[46] H.W. Trissl, J. Lavergne, Theory of fluorescence induction in photosystem II: derivation of analytical expressions in a model including exciton-radical-pair equilibrium and restricted energy transfer between photosynthetic units, Biophys. J. 68 (1995) 2474–2492.
[47] R. Delosme, P. Joliot, Period four oscillations in chlorophyll a fluorescence, Photosynth. Res. 73 (2002) 165–168.
[48] B.-D. Hsu, Evidence for the contribution of the S-state transitions of oxygen evolution to the initial phase of fluorescence induction, Photosynth. Res. 36 (1993) 81–88.